Talanta 129 (2014) 545–551

Contents lists available at ScienceDirect

Talanta

journal homepage: www.elsevier.com/locate/talanta

Impedimetric detection of alcohol vapours using nanostructured zinc ferrite

Padmanathan Karthick Kannan, Ramiah Saraswathi *

Department of Materials Science, School of Chemistry, Madurai Kamaraj University, Madurai 625021, India

ARTICLE INFO

Article history:
Received 21 March 2014
Received in revised form
12 June 2014
Accepted 13 June 2014
Available online 24 June 2014

Keywords:
Impedimetric sensor
Alcohol sensor
Zinc ferrite
Combustion method
Equivalent circuit modelling

ABSTRACT

A comparative study on the sensing characteristics of nanostructured zinc ferrite to three primary alcohols *viz*. methanol, ethanol and propanol has been carried out. The zinc ferrite has been prepared by a combustion method and characterized by XRD, FTIR, AFM and SEM. Impedance studies in the alcohol concentration range varying from 100 to 1000 ppm show definite variations in response to both the nature of the alcohol and its concentration. The nanostructured zinc ferrite shows the highest sensor response to methanol and least to propanol. Equivalent circuit modelling and calibration have been made for all the three alcohol sensors. The material shows a better selectivity to the alcohols compared to formaldehyde, ammonia and acetone vapours.

1. Introduction

Aliphatic alcohols like methanol, ethanol and propanol have been widely used in various industrial and scientific applications [1–3]. Methanol is a very useful organic solvent with widespread applications in automotive fuels and also it is used in the manufacturing of dyes, drugs and perfumes [4]. However, it is highly toxic and seriously hazardous to human health [5]. Ethanol is a hypnotic solvent and it is widely applied in wine making, medical processes and food industries. A continuous monitoring of ethanol is required in wine industry in order to determine the quality and special flavour of wine. Also, ethanol has to be measured in breath analysis [6]. Propanol is used as a solvent for several organic compounds. It is widely used as a cleaning fluid, especially for dissolving oils. Propanol is a skin irritant and its long term exposure can lead to a series of health complications [7]. Hence there is a great demand for monitoring the three primary alcohol vapours.

Nanostructured materials including metal oxides, carbon nanotubes, graphene and conducting polymer–nanocarbon composites are being vigorously explored in chemical gas sensors [8–12]. Owing to their small grain size, high density of grain boundaries and interfaces, nanostructured materials are expected to show a strong reactivity towards gases and organic vapours. The high surface area together with the potential to control the microstructure make nanomaterials very attractive for the development of highly sensitive gas sensors with fast response [13]. In particular, nanostructured metal oxides like SnO_2, ZnO, Fe_2O_3 and WO_3 have been widely used in alcohol sensing [14–17]. Many of the studies report that these binary metal oxides exhibit a high sensitivity to ethanol compared to other alcohols [18–20]. However, they are also known to suffer from poor selectivity and high working temperature [21].

Recently, nanostructured ferrite materials have received considerable attention in gas sensor application as they exhibit more selectivity and stability for a particular gas than simple metal oxides [22]. Ferrites offer several advantages which include the ability to tune the electrical properties by varying the cation composition and annealing condition [23]. Among the various ferrite materials, zinc ferrite is an important n-type semiconducting material widely applied for the detection of acetone, ethanol, hydrogen and H_2S because of its good chemical and thermal stability [24–28]. Its simple preparation, low cost and high reactivity to chemical species make it a highly suitable material for use in gas sensors.

The present study is aimed to develop an impedimetric sensor for the detection of three primary alcohols *viz*. methanol, ethanol and propanol using nanostructured zinc ferrite. It may be mentioned here that the alcohol sensors hitherto reported in the literature are either of chemiresistive-type or based on optical methods [29,30]. Recently, there have been some interesting reports on the use of impedance spectroscopy as a calibration tool in the detection of some organic vapours and polluting gases [31–34]. Impedance technique has several advantages compared to conventional gas sensing methods. The high precision method measures the response of a system to the application of a periodic small amplitude ac signal at a wide range of frequencies. The

* Corresponding author. Tel.: +91 452 2458247; fax: +91 452 2459181.
E-mail address: drrsaraswathi@gmail.com (R. Saraswathi).

http://dx.doi.org/10.1016/j.talanta.2014.06.028
0039-9140/

analysis of the impedance data yields useful information about the physicochemical properties of the system [35,36]. It is a very powerful tool to examine the nature of conduction processes and the mechanism of solid/gas interactions as the processes of different time constants can be distinguished by varying the frequency [37]. Further, equivalent circuit modelling of the impedance data provides an understanding of the device structure. In addition, it helps to distinguish between the contributions from the bulk, grain boundary and electrode and to determine the factors influencing the sensitivity of the gas sensor [38]. To the best of our knowledge, there has been no report yet on an impedimetric alcohol sensor and herein we present a comparative study on the sensing characteristics of nanostructured zinc ferrite towards methanol, ethanol and propanol using impedance technique at room temperature.

2. Experimental

2.1. Preparation of nanostructured zinc ferrite

An aqueous combustion method was used to prepare nanostructured zinc ferrite. Typically the combustion technique involves a self-sustained reaction in solutions of metal nitrates (oxidizer) and organic fuels and it is a convenient and cost-effective method to obtain nanostructured ferrites with high yield and phase purity [39]. In this study nanopowder of zinc ferrite was synthesized using zinc nitrate and iron nitrate as the precursor materials and citric acid as the fuel source. 100 mL aqueous solution containing zinc nitrate (2.98 g), iron nitrate (8.08 g) and citric acid (4.20 g) was heated to about 250 °C. Water was evaporated until the solution became a viscous-gel due to the dehydration process. Persistent heating led to the formation of a reddish yellow coloured product. This as-prepared sample was then annealed at 700 °C for 2 h to get a pure and crystalline zinc ferrite nanopowder.

2.2. Characterization

X-ray diffraction pattern was obtained using an XPERT-PRO PANalytical diffractometer with CuKα radiation ($\lambda = 1.5406$ Å). The IR spectrum was recorded using a FT-IR spectrometer (Shimadzu 8400S). The morphology of the samples was examined by a scanning electron microscope (Hitachi S-3000H, Japan). The surface topography was obtained using an atomic force microscope (APE Research Model A100 SGS). Impedance measurements were carried out using a EG&G potentiostat/galvanostat model 2273, USA. The electrical parameters were determined by fitting the impedance spectra using the ZSimpWin 3.21 software.

2.3. Sensor fabrication and measurements

About 60 mg of the zinc ferrite sample was pressed into a pellet (13 mm dia and 0.3 mm thickness) by applying a pressure of 5 t/cm^2. A two-probe method was used for sensor measurements. The electrical leads were taken 0.2 cm apart using two thin copper wires with the help of conductive silver paste on the surface of the pellet. The pellet was then placed in a glass chamber of volume 1000 mL. The volume of alcohol (V, μL) required to achieve a specific vapour concentration in ppm inside the test chamber was obtained using the relation [40]

$$V = \frac{CV_a M}{(2.46 \times 10^7) \times D} \quad (1)$$

where C is the required gas concentration (ppm), V_a is the volume of air which is equal to the volume of test chamber (mL), M is the molecular weight of alcohol (g/mol) and D is the density of the alcohol (g/mL). The alcohol sensing properties of the pellet were investigated by injecting the desired concentration of alcohol into the glass chamber. After allowing sufficient time for equilibrium, the electrical impedance was measured in the frequency range between 1 Hz and 1 MHz. The sensor response was calculated using the relation [41–44]

$$\text{Sensor response} = \frac{|Z_a|}{|Z_g|} \quad (2)$$

where $|Z_a|$ and $|Z_g|$ are the moduli of the impedance values in air and in the presence of alcohol at a defined frequency value.

3. Results and discussions

3.1. Structural and morphological characterization

The XRD pattern (Fig. 1) of the nanostructured zinc ferrite synthesized by the combustion method and annealed at 700 °C for 2 h shows sharp and high intensity peaks indicating that the sample exhibits high order of crystallinity. The peaks could be indexed to the (111), (220), (311), (222), (400), (422), (511), (440), (620) and (533) planes of cubic zinc ferrite [45]. The lattice constant is calculated to be 8.43 Å. Based on the full width at half-maximum value of all the peaks, the average grain size is calculated to be 47 nm using the Debye–Scherrer equation [46].

The FTIR spectrum of nanostructured zinc ferrite is shown in Fig. 2. The absorption bands at 543 and 395 cm^{-1} can be ascribed to the stretching vibrations of Fe–O bond and Zn–O bond present in the octahedral and tetrahedral sites of zinc ferrite respectively [47]. The absence of any other band in the spectrum suggests the formation of a pure product of zinc ferrite.

The SEM image of the nanostructured zinc ferrite sample (Fig. 3A) shows the presence of multigrain agglomerations with discrete crystallites. The existence of voids indicates a porous microstructure which will be advantageous to the gas sensing application. Fig. 3B and C shows the 2D and 3D AFM images of zinc ferrite which indicate the presence of spherical particles of about 51 nm diameter.

3.2. Alcohol sensor characterization

At first, for reference, the complex impedance plot was measured in air which shows an arc with a large curvature radius

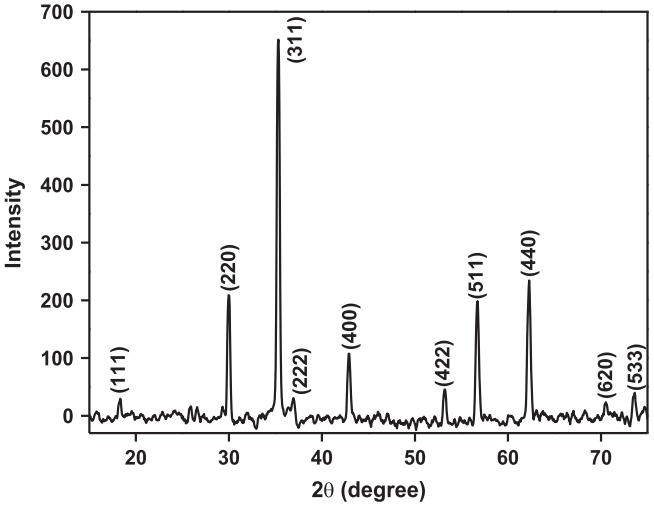

Fig. 1. XRD pattern of nanostructured zinc ferrite.

between 1 KHz and 1 MHz (inset of Fig. 4A). Fig. 4A–C shows the complex impedance plots obtained when the zinc ferrite pellet was exposed to methanol, ethanol and propanol in the concentration range between 100 and 1000 ppm. For all the three alcohols, the impedance plots at low concentrations (<200 ppm) show an inclined arc in the frequency range between 1 Hz and 1 MHz. When the concentration of alcohol is increased, the radius of curvature of the arc is reduced and the plot shows two overlaid semicircles implying the prevalence of a mixed charge transport mechanism involving grains and grain boundaries with different relaxation times. The semicircle in the low frequency region can be ascribed to the grain boundary area while that in the high frequency is associated with the grain interior region [48]. The significant observation is a finite decrease in the complex impedance when the zinc ferrite is exposed to the alcohol vapour. A two order impedance variation is observed for methanol while one `order variation is observed for ethanol and propanol in the alcohol concentration range investigated (Fig. S1 in electronic Supplementary information).

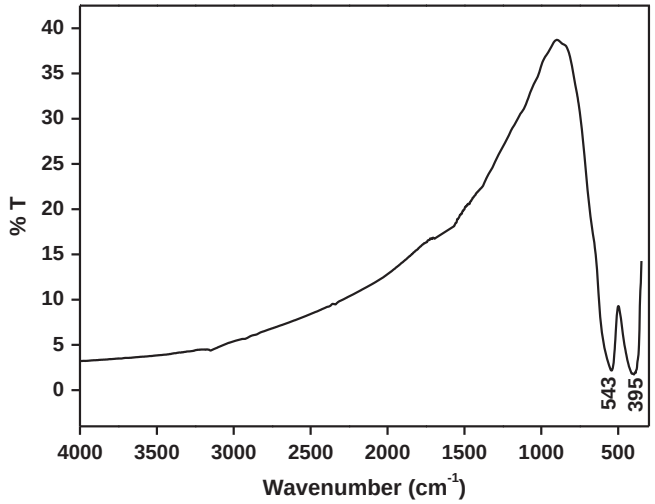

Fig. 2. FTIR spectrum of nanostructured zinc ferrite.

The mechanism of sensing of alcohol by the n-type zinc ferrite can be explained on the basis of oxygen ionosorption model [49,50]. Accordingly, oxygen molecules physisorbed on the surface of zinc ferrite will capture free electrons from its conduction band to form ionosorbed oxygen species (Eqs. (3)–(6)). The nature of ionosorbed oxygen on the surface will vary depending upon the sensor operating temperature. If the sensor operating temperature is below 150 °C, the molecular form (O_2^-) dominates and if the operating temperature is above 150 °C, the atomic form (O^-) dominates [51,52].

$$\text{Physisorption}: O_{2(gas)} \rightarrow O_{2(ads)} \quad (3)$$

$$\text{Ionosorption}: O_{2(ads)} + e^- \rightarrow O^-_{2(ads)} \quad RT - 150\ ^\circ C \quad (4)$$

$$O^-_{2(ads)} + e^- \rightarrow 2O^-_{(ads)} \quad 150 - 300\ ^\circ C \quad (5)$$

$$2O^-_{(ads)} + e^- \rightarrow O^{2-}_{(ads)} \quad > 300\ ^\circ C \quad (6)$$

Considering the fact that the present data are obtained at room temperature, the O_2^- is the most likely species to interact with the alcohol molecules (Eqs. (7)–(9)) [53, 54] releasing the trapped

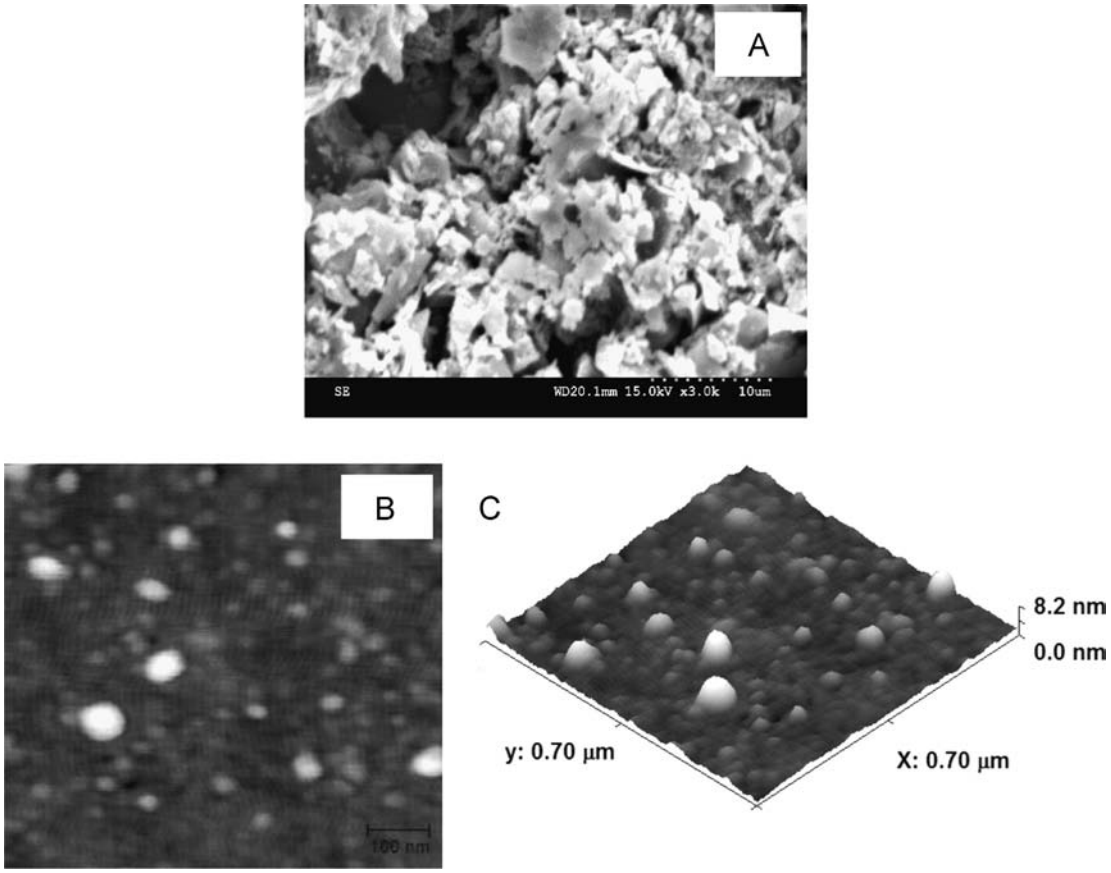

Fig. 3. (A) SEM image of zinc ferrite sample. (B) 2D and (C) 3D AFM images of zinc ferrite sample.

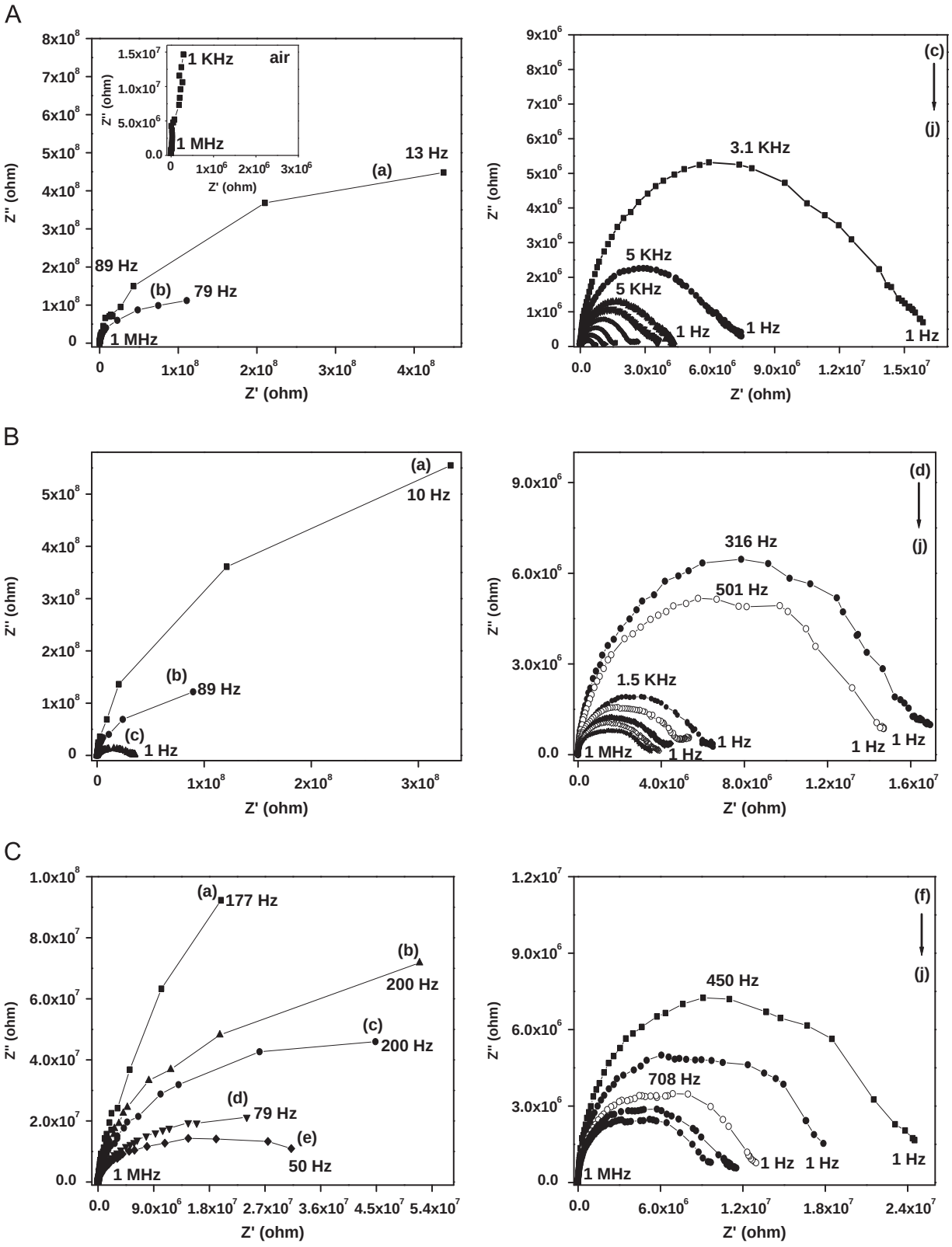

Fig. 4. Complex impedance plots of zinc ferrite at different concentrations of alcohols: (A) methanol (B) ethanol and (C) propanol. (a) 100 ppm (b) 200 ppm (c) 300 ppm (d) 400 ppm (e) 500 ppm (f) 600 ppm (g) 700 ppm (h) 800 ppm (i) 900 ppm (j) 1000 ppm. Inset(A) shows the complex impedance plot of zinc ferrite measured in air.

electrons back to the conduction band and this will eventually lead to a decrease in the impedance value of zinc ferrite. As the concentration of alcohol is increased, there will be a rapid depletion of O_2^- on the surface and increase of the electron concentration causing a considerable decrease in the electrical impedance.

$$CH_3OH + O_2^- \rightarrow HCOOH + H_2O + e^- \quad (7)$$

$$2C_2H_5OH + O_2^- \rightarrow 2CH_3CHO + 2H_2O + e^- \quad (8)$$

$$CH_3CH_2CH_2OH + O_2^- \rightarrow CH_3CH_2COOH + H_2O + e^- \quad (9)$$

In order to derive further understanding of the electrical behaviour and the charge transport processes contributing to variation in response to the nature and concentration of alcohol, the experimental impedance data were analysed by equivalent circuit modelling [55]. The impedance data obtained in air and at lower concentrations of alcohols i.e., ≤ 200 ppm for methanol and ethanol and ≤ 300 ppm for propanol can be well fitted to an equivalent circuit constituted by one resistance with a parallel capacitance elements (Fig. 5A). However, at higher concentrations, the observed impedance data with two overlaid semicircles can be

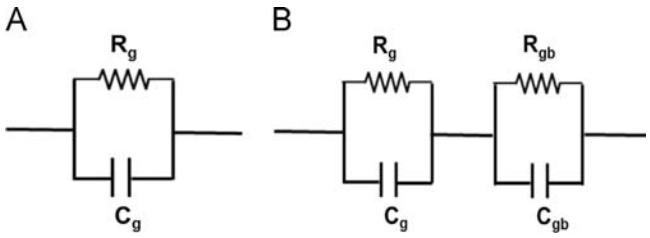

Fig. 5. Electrical circuits used for modelling of impedance data measured in (A) air and in ≤ 200 ppm for methanol and ethanol, ≤ 300 ppm for propanol and (B) at alcohol concentration ≥ 300 ppm.

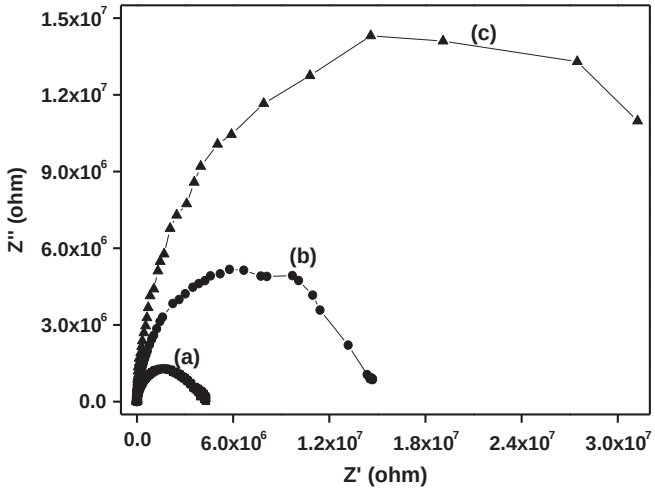

Fig. 6. Complex impedance spectra of zinc ferrite sensor measured in 500 ppm of (a) methanol (b) ethanol (c) propanol.

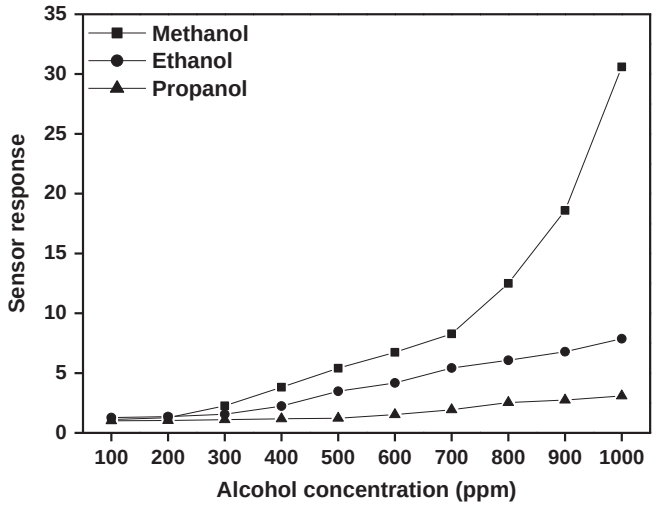

Fig. 7. Plot of sensor response against alcohol concentration for zinc ferrite pellet sensor in the entire measured range.

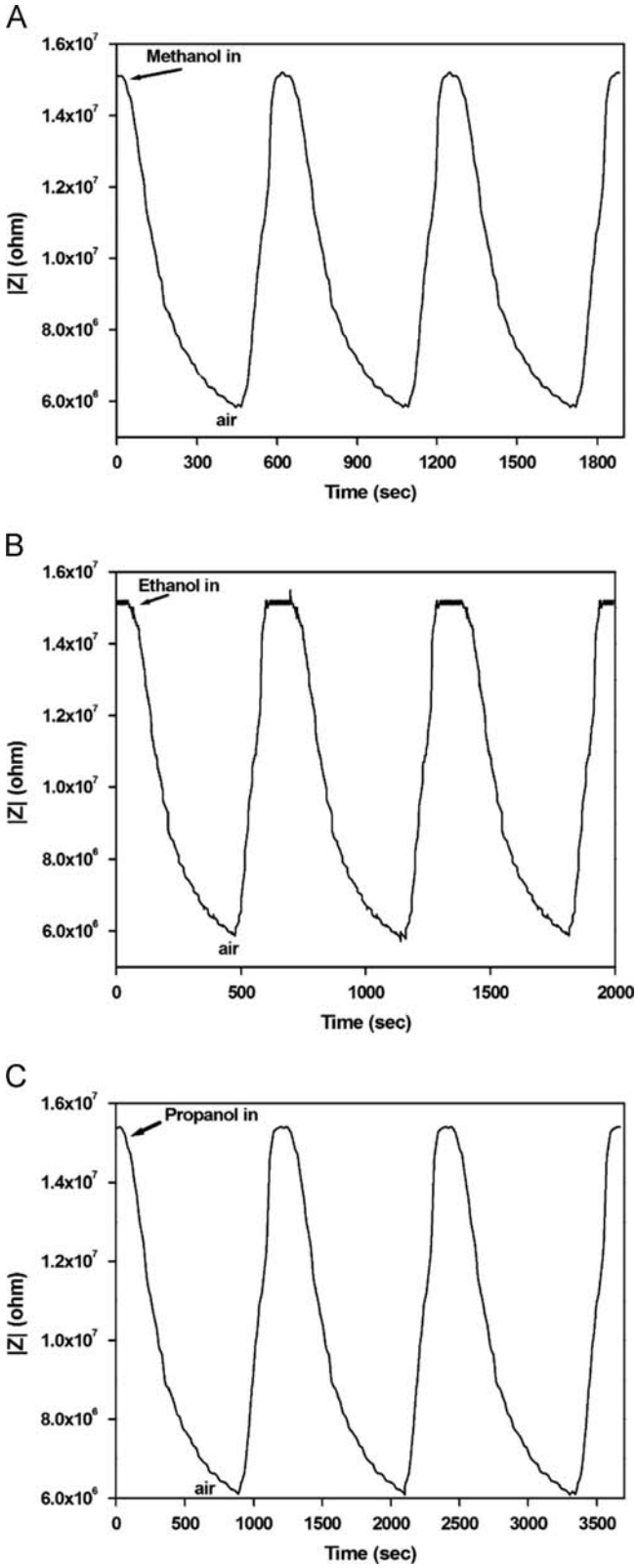

Fig. 8. Dynamic response of zinc ferrite pellet sensor during adsorption–desorption of alcohols at 300 ppm: (a) methanol (b) ethanol and (c) propanol.

fitted to an equivalent circuit consisting of two resistances with parallel capacitance components (Fig. 5B).

The impedance parameters extracted from the equivalent circuit modelling for the three alcohols are given in Tables S1–S3 (see electronic Supplementary information). The resistance in the high frequency region is attributed to the grain interior or bulk resistance (R_g) while that corresponding to the low frequency region is due to the grain boundary resistance (R_{gb}) [56,57]. It is observed that both R_g and R_{gb} decrease with increasing concentration for all three alcohols but their absolute magnitudes and order of variation in the measured concentration range are quite different.

In order to derive information on the alcohol to which zinc ferrite shows the maximum sensor response, a comparison of the impedance plots at 500 ppm of each of the three alcohols is made (Fig. 6). A clear difference in the impedance spectra can be observed in that the diameter of the semicircle (R_{ct}, charge transfer resistance) shows a three order variation for methanol, whereas in the presence of ethanol and propanol, a two order variation is observed in the measured concentration range (Tables S1–S3 in electronic Supplementary information). Also, the maximum value of the imaginary impedance (Z'') at the relaxation frequency vary in the order:

Methanol < Ethanol < Propanol

The variation in sensor response against the alcohol concentration from 100 to 1000 ppm is shown in Fig. 7. It can be observed that for all the three alcohols, the sensor response increases with increase in concentration. The sensor response value is increased from 1.12 to 30.6 when the methanol concentration is increased from 100 to 1000 ppm. Similarly for ethanol, the sensor response value increases from 1.28 at 100 ppm to 7.87 at 1000 ppm. Likewise, for propanol, the response value increases from 1.01 to 3.09 when the concentration is increased from 100 to 1000 ppm.

These results imply the different physical phenomena of electrical conduction and polarization occurring in zinc ferrite in the presence of the alcohol molecules. The low molecular weight and high polarity of the methanol in comparison to ethanol and propanol perhaps lead to an increased reactivity with zinc ferrite resulting in a low impedance value [58,59]. Therefore, it is inferred that zinc ferrite shows a greater sensitivity to methanol compared to ethanol and propanol.

Fig. 8 shows the response–recovery curves of the zinc ferrite pellet sensor obtained at 300 ppm of methanol, ethanol and propanol at a frequency value of 1 KHz. From the data, the response and recovery time values of the sensor are calculated and shown in Table 1. Methanol shows the lowest response and recovery time while propanol shows nearly twice the values. The stability data of the three alcohol sensors obtained under similar conditions at room temperature over a period of 30 days with a time interval of 5 days confirm the reliability of the measurements (Fig. 9).

The selectivity of the 700 °C annealed zinc ferrite pellet has been studied by exposing the pellet to 300 ppm of various vapours such as acetone, ammonia and formaldehyde. The results are shown in Fig. 10 which clearly indicate that zinc ferrite shows the highest sensitivity to alcohols compared to other reducing vapours. It is also found from the plot that the pellet sensor shows maximum sensitivity to methanol under the optimized conditions.

Table 1
Response–recovery data of zinc ferrite sensor at 300 ppm of methanol, ethanol and propanol.

Alcohol	Response time (min)	Recovery time (min)
Methanol	4.60	2.00
Ethanol	4.75	2.78
Propanol	8.00	5.00

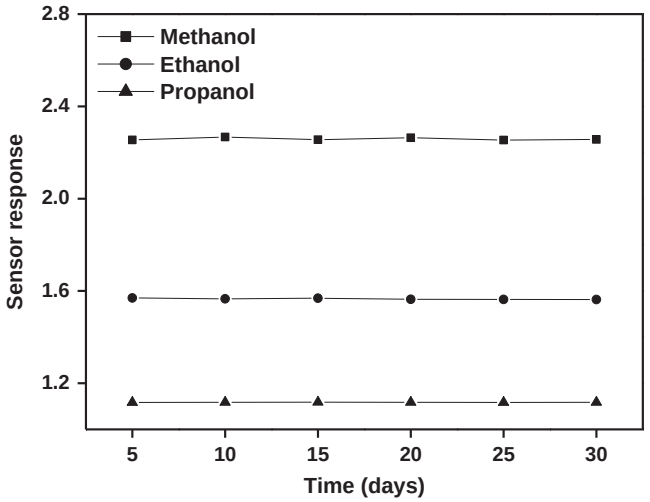

Fig. 9. Stability data of zinc ferrite pellet sensor in 300 ppm of (■) methanol (●) ethanol and (▲) propanol.

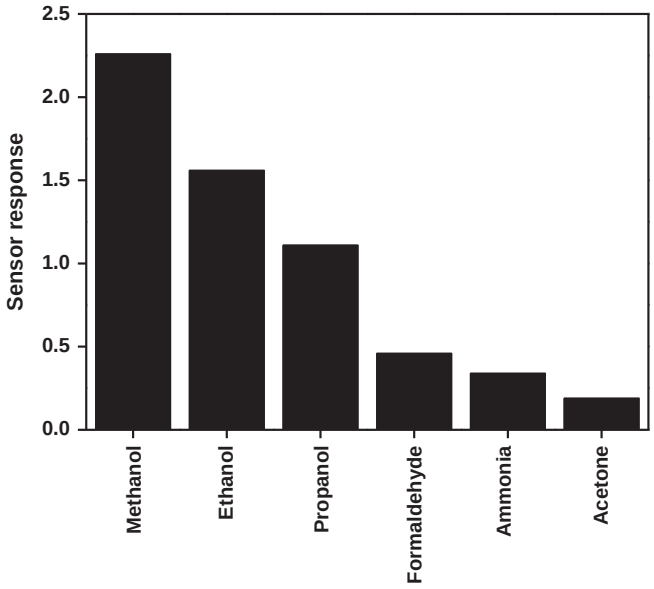

Fig. 10. A bar diagram showing the sensor response of zinc ferrite pellet sensor towards various reducing vapours each at a concentration of 300 ppm.

4. Conclusions

Nanostructured zinc ferrite has been prepared by the aqueous combustion method and the sample is systematically characterized by XRD, SEM, AFM and FTIR techniques. An impedimetric zinc ferrite-based sensor has been developed for the detection of three primary alcohols *viz*. methanol, ethanol and propanol. The comparative study shows that the material is more specific to alcohols especially to the detection of methanol with high sensitivity, quick response and good stability.

Acknowledgment

Financial assistance from University Grants Commission, New Delhi, Government of India under the University with Potential for Excellence Scheme to Madurai Kamaraj University is gratefully acknowledged.

Appendix A. Supporting information

Supplementary data associated with this article can be found in the online version at http://dx.doi.org/10.1016/j.talanta.2014.06.028.

References

[1] G.A. Olah, Angew. Chem. Int. Ed. 44 (2005) 2636–2639.
[2] T. Yarita, R. Nakajima, S. Otsuka, T. Ihara, A. Takatsu, M. Shibukawa, J. Chromatogr. A 976 (2002) 387–391.
[3] S.-H. Park, Y.-Y. Kim, K.-W. Lee, Sens. Actuators B 176 (2013) 437–442.
[4] N.G. Patel, P.D. Patel, V.S. Vaishnav, Sens. Actuators B 96 (2003) 180–189.
[5] M.L. Frenia, J.L. Schauben, Ann. Emerg. Med. 22 (1993) 1919–1923.
[6] M. Niculescu, T. Erichsen, V. Sukharev, Z. Kerenyi, E. Csoregi, W. Schuhmann, Anal. Chim. Acta 463 (2002) 39–51.
[7] M.A.M. Smeets, C. Maute, P.H. Dalton, Ann. Occup. Hyg. 46 (2002) 359–373.
[8] M. Ahsan, M.Z. Ahmad, T. Tesfamichael, J. Bell, W. Wlodarski, N. Motta, Sens. Actuators B 173 (2012) 789–796.
[9] F. Rumiche, H.H. Wang, J.E. Indacochea, Sens. Actuators B 163 (2012) 97–106.
[10] N. Hu, Z. Yang, Y. Wang, L. Zhang, Y. Wang, X. Huang, H. Wei, L. Wei, Y. Zhang, Nanotechnology 25 (2014) 025502.
[11] C. Wei, L. Dai, A. Roy, T.B. Tolle, J. Am. Chem. Soc. 128 (2006) 1412–1413.
[12] M. Parmar, C. Balamurugan, D.W. Lee, Sensors 13 (2013) 16611–16624.
[13] G.J. Cadena, J. Riu, F.X. Rius, Analyst 132 (2007) 1083–1099.
[14] H.C. Chiu, C.S. Yeh, J. Phys. Chem. C 111 (2007) 7256–7259.
[15] Y.J. Chen, C.L. Zhu, G. Xiao, Sens. Actuators B 129 (2008) 639–642.
[16] L. Wang, T. Fei, Z. Lou, T. Zhang, ACS Appl. Mater. Interfaces 3 (2011) 4689–4694.
[17] D. Chen, X. Hou, H. Wen, Y. Wang, H. Wang, X. Li, R. Zhang, H. Lu, H. Xu, S. Guan, J. Sun, L. Gao, Nanotechnology 21 (2010) 035501.
[18] E. Comini, G. Faglia, G. Sberveglieri, D. Calestani, L. Zanotti, M. Zhab, Sens. Actuators B 111–112 (2005) 2–6.
[19] H.J. Pandya, S. Chandra, A.L. Vyas, Sens. Actuators B 161 (2012) 923–928.
[20] P. Ivanov, E. Llobet, X. Vilanova, J. Brezmes, J. Hubalek, X. Correig, Sens. Actuators B 99 (2004) 201–206.
[21] N. Coppede, M. Villani, R. Mosca, S. Iannotta, A. Zappettini, D. Calestani, Sensors 13 (2013) 3445–3453.
[22] A.B. Gadkari, T.J. Shinde, P.N. Vasambekar, IEEE Sens. J. 11 (2011) 849–861.
[23] A. Sutka, G. Mezinskis, A. Lusis, M. Stingaciu, Sens. Actuators B 171-172 (2012) 354–360.
[24] A. Sutka, J. Zavickis, G. Mezinskis, D. Jakovlevs, J. Barloti, Sens. Actuators B 176 (2013) 330–334.
[25] K. Mukherjee, S.B. Majumder, J. Appl. Phys. 106 (2009) 064912.
[26] S.L. Darshane, R.G. Deshmukh, S.S. Suryavanshi, I.S. Mulla, J. Am. Ceram. Soc. 91 (2008) 2724–2726.
[27] Y. Cao, D. Jia, P. Hu, R. Wang, Ceram. Int. 39 (2013) 2989–2994.
[28] G. Zhang, C. Li, F. Cheng, J. Chen, Sens. Actuators B 120 (2007) 403–410.
[29] J. Ima, S.K. Sengupta, M.F. Baruch, C.D. Granz, S. Ammu, S.K. Manohar, J. E. Whitten, Sens. Actuators B 156 (2011) 715–722.
[30] M. Morisawa, S. Muto, J. Sens. (2012) (Article ID 709849).
[31] L. Liu, X. Li, P.K. Dutta, J. Wang, Sens. Actuators B 185 (2013) 1–9.
[32] Z. Ling, C. Leach, R. Freer, Sens. Actuators B 87 (2002) 215–221.
[33] M. Stranzenbach, B. Saruhan, Sens. Actuators B 137 (2009) 154–163.
[34] P.K Kannan, R. Saraswathi, J. Mater, Chem. A 2 (2014) 394–401.
[35] J.R. Macdonald, Ann. Biomed. Eng. 20 (1992) 289–305.
[36] F.G. Banica, Chemical Sensors and Biosensors: Fundamentals and Applications, John Wiley & Sons, Chichester (2012) 367–403.
[37] R. Lalauze, Chemical Sensors and Biosensors, John Wiley & Sons, Hoboken (2012) 143–174.
[38] M. Kaur, S.K. Gupta, C.A. Betty, V. Saxena, V.R. Katti, S.C. Gadkari, J.V. Yakhmi, Sens. Actuators B 107 (2005) 360–365.
[39] S. Castro, M. Gayoso, C. Rodriguez, J. Solid State Chem. 134 (1997) 227–231.
[40] L. Peng, P. Qin, Q. Zeng, H. Song, M. Lei, J.J.N. Mwangi, D. Wang, T. Xie, Sens. Actuators B 160 (2011) 39–45.
[41] J.M. Rheaume, A.P. Pisano, Ionics 17 (2011) 99–108.
[42] R. Mariappan, V. Ponnuswamy, R. Suresh, P. Suresh, A. Chandrabose, M. Raghavendar, J. Alloys Compd. 582 (2014) 387–391.
[43] M. Kashif, M.E. Ali, S.M.U. Ali, U. Hashim, S.B.A. Hamid, Nanoscale Res. Lett. 8 (2013) 68.
[44] N.H. Al-Hardan, M.J. Abdullah, A.Abdul Aziz, Int. J. Hydrog. Energy 35 (2010) 4428–4434.
[45] JCPDS Card No. 22-1012, International Centre for Diffraction Data, Newtown Square, PA, USA.
[46] V.K. Pecharsky, P.Y. Zavalij, Fundamentals of Powder Diffraction and Structural Characterization of Materials, Second ed., Springer, New York, 2009.
[47] A. Pradeep, P. Priyadharsini, G. Chandrasekaran, J. Alloys Compd. 509 (2011) 3917–3923.
[48] C.R. Bowen, A.W. Tavernor, J. Luo, R. Stevens, J. Eur. Ceram. Soc. 19 (1999) 149–154.
[49] A. Gurlo, Chem. Phys. Chem. 7 (2006) 2041–2052.
[50] U. Pulkkinen, T.T. Rantala, T.S. Rantala, V. Lantto, J. Mol. Catal. A: Chem. 166 (2001) 15–21.
[51] H. Liu, S.P. Gong, Y.X. Hu, J.Q. Liu, D.X. Zhou, Sens. Actuators B 140 (2009) 190–195.
[52] P.V. Bakharev, V.V. Dobrokhotov, D.N. McIlroy, Chemosensors 2 (2014) 56–68.
[53] M.M. Rahman, S.B. Khan, A. Jamal, M. Faisal, A.M. Asiri, Microchim. Acta 178 (2012) 99–106.
[54] C.S. Prajapati, P.P. Sahay, Sens. Actuators B 160 (2011) 1043–1049.
[55] I.I. Suni, Trends Anal. Chem. 27 (2008) 604–611.
[56] U. Weimar, W. Gopel, Sens. Actuators B 26–27 (1995) 13–18.
[57] S. Sen, K.P. Muthe, N. Joshi, S.C. Gadkari, S.K. Gupta, J.M. Roy, S.K. Deshpande, J. V. Yakhmi, Sens. Actuators B 98 (2004) 154–159.
[58] M. Vrnata, V. Myslik, F. Vyslouil, M. Jelinek, J. Lancok, J. Zemek, Sens. Actuators B 71 (2000) 24–30.
[59] G.S. Aluri, A. Motayed, A.V. Davydov, V.P. Oleshko, K.A. Bertness, N.A. Sanford, R.V. Mulpuri, Nanotechnology 23 (2012) 175501–175512.